Chinese Journal of
POLYMER SCIENCE

RESEARCH ARTICLE

https://doi.org/10.1007/s10118-024-3152-2
Chinese J. Polym. Sci.

Swelling of Spherical Polyelectrolyte Gels

Ming-Yu Duan, Jia-Dong Chen, Yi-Ming Liu, Zhao-Feng Peng, and Guang Chen*

Department of Advanced Manufacturing and Robotics, College of Engineering, Peking University, Beijing 100871, China

Abstract Polyelectrolyte (PE) gels, distinguished by their unique stimuli-responsive swelling behavior, serve as the basis of broad applications, such as artificial muscles and drug delivery. In this work, we present a theoretical model to analyze the electrostatics and its contribution to the swelling behavior of PE gels in salt solutions. By minimizing the free energy of PE gels, we obtain two distinct scaling regimes for the swelling ratio at equilibrium with respect to the salt concentration. We compare our predictions for the swelling ratio with experimental measurements, which show excellent agreement. In addition, we employ a finite element method to assess the applicability range of our theoretical model and assumptions. We anticipate that our model will also provide valuable insights into drug adsorption and release, deformation of red blood cells, 4D printing and soft robotics, where the underlying mechanism of swelling remains enigmatic.

Keywords Gels; Polyelectrolytes; Swelling; Stimuli-responsive; Electrostatic interaction; Cell model

Citation: Duan, M. Y.; Chen, J. D.; Liu, Y. M.; Peng, Z. F.; Chen, G. Swelling of spherical polyelectrolyte gels. *Chinese J. Polym. Sci.* https://doi.org/10.1007/s10118-024-3152-2

INTRODUCTION

Polyelectrolyte (PE) gels are a special kind of hydrogels, which contain charged polymer networks arising from the ionization of monomers.[1] PE gels are found to exhibit unique swelling behavior in response to ambient factors including salt concentration and pH value, owing to the electrostatic interactions.[2,3] As a result, the stimuli-responsive swelling of PE gels holds significant potential for broad applications in soft robotics, biomedicine, and advanced manufacturing, such as artificial muscles[4,5], drug delivery[6,7] and 4D printing.[8,9]

Over the past few decades, significant progress has been made in comprehending and modelling the swelling of PE gels. The pioneer work of Flory and Rehner[10,11] establishes the free energy function of polymer gels, with assumptions are further clarified by Tanaka.[12] The Flory-Rehner framework encompasses contributions from the polymer chain-solvent mixing and the entropy of deformation. Subsequent studies aimed to understand the swelling of charged PE gels by incorporating additional contributions from electrostatic interactions among charged monomers and mobile ions.[13–22] However, the electrostatics is often oversimplified, since a priori assumptions are made which consider the bulk salt concentration as the summation of the mean average counterion concentration and the added salt concentration. In this work, we develop a new theory to characterize the electrostatic interactions among the charged monomers and their surrounding mobile ions in the PE gels. We aim to provide both qualitative and quantitative explanations of the swelling behavior of PE gels in salt solutions. We also compare our predictions with experiments and discuss the range of applicability of our model.

THEORY

We consider a spherical PE gel immersed in an aqueous solution with a salt concentration of n_s, as shown in Fig. 1(a). After free swelling, the PE gel reaches a volume of V at the equilibrium state. Here, we consider that the total free energy F of the PE gel is contributed by the elastic (els) free energy F_{els} and electrostatic (elec) free energy F_{elec},

$$\frac{F}{k_{\text{B}}T} = \frac{F_{\text{els}}}{k_{\text{B}}T} + \frac{F_{\text{elec}}}{k_{\text{B}}T} \tag{1}$$

where k_{B} represents the Boltzmann constant and T is the thermodynamic temperature. The elastic free energy F_{els} of the spherical PE gel can be described by the neo-Hookean model,

$$\frac{F_{\text{els}}}{k_{\text{B}}T} = \frac{3}{2}\frac{G_0V_0}{k_{\text{B}}T}\left(\frac{V}{V_0}\right)^{\frac{2}{3}} \tag{2}$$

where V_0 and G_0 denote the volume and shear modulus of the PE gel at the reference state, respectively.[23] Note that Eq. (2) is applicable as long as the PE segments follow the Gaussian statistics in the weak swelling regime ($V/V_0 < 10$). For the scenario of high swelling, the finite extensibility effect on the chain elasticity should be taken into account.[24]

The electrostatic free energy F_{elec} is attributed to the electrostatic interactions among the PE chains and their surrounding mobile ions, as well as the entropy of mixing of all the ions, as shown in Fig. 1(b). We consider that the PE gel

* Corresponding author, E-mail: guangc@pku.edu.cn

Special Issue: Charged Polymers
Received April 11, 2024; Accepted April 30, 2024; Published online June 6, 2024

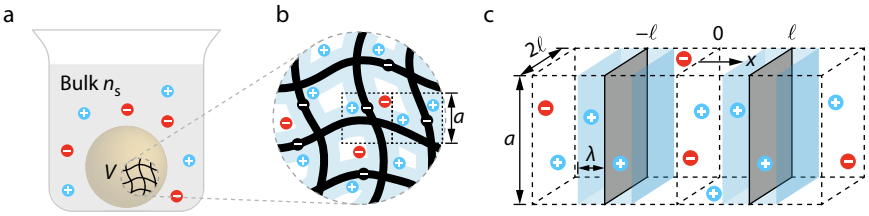

Fig. 1 (a) Schematic illustrating a spherical PE gel immersed in a monovalent salt solution. (b) Zoom-in illustration showcasing the electrostatic interactions among mobile ions and charged monomers. (c) Cell model depicting two adjacent monomers for modelling the electrostatic interactions.

contains totally N_t monomers, and the charge fraction is φ. To quantify the electrostatic free energy F_{elec} of the PE gel, we employ a cell model,[25,26] which divides the PE gel into N_t cells, as depicted in Fig. 1(c). We assume that the monomers are homogeneously distributed within the gel, so that each cell contains one monomer of size a and has the same volume $\Omega = V/N_t$. Accordingly, the cell size is $2\ell = \sqrt{V/(aN_t)}$. We model the negatively charged monomers as similarly charged plates with the surface charge density $\sigma = -e\varphi/A$, where e is the elementary charge and $A = 4\ell a$ is the surface area of the plate in each cell. The electric double layers (EDLs) are formed near the charged plates, where the thickness can be characterized by the Debye length $\lambda = \sqrt{\varepsilon_0\varepsilon_r k_B T/(2e^2 n_s)}$, as shown in Fig. 1(c). Here, ε_0 and ε_r are the vacuum permittivity and relative dielectric constant of water, respectively. With our notation, the electrostatic free energy F_{elec} of the PE gel is

$$\begin{aligned}\frac{F_{elec}}{k_B T} =& N_t \int_A \frac{\sigma\psi_s}{k_B T} dA + N_t \int_\Omega -\frac{\varepsilon_0\varepsilon_r}{2k_B T}|\nabla\psi|^2 d\Omega \\ &+ N_t \int_\Omega \sum_i \left\{ \frac{e\psi}{k_B T} z_i n_i + n_{i,\infty} + n_i \left[\ln\left(\frac{n_i}{n_{i,\infty}}\right) - 1 \right] \right\} d\Omega \end{aligned} \tag{3}$$

where ψ is the electrostatic potential relative to a reference $\psi = 0$ in the bulk, ψ_s is the electrostatic potential at the charged surface (S), i denotes the ion species, z_i is the valence of ions, and n_i and $n_{i,\infty}$ are the local and bulk ion concentrations, respectively.

The swelling ratio V/V_0 of the PE gel, corresponding to the minimum of total free energy F (*i.e.*, $\delta F/\delta V = 0$), can be obtained analytically and numerically using Eqs. (1)–(3).

EXPERIMENTAL

We use sodium chloride (NaCl, 99%) purchased from Sigma-Aldrich to prepare the salt solutions. The salt was directly dissolved in Wahaha DI water (Wahaha Corp., China) to prepare 1 mol/L solutions, which were then diluted to obtain 10^{-1}, 10^{-2}, 10^{-3} and 10^{-4} mol/L solutions for experiments. Two kinds of dry spherical polymer beads were purchased from e-commerce platform, where one is more rigid and smaller than the other. The dry PEGel-1 beads have an average weight of 0.006 g and an average diameter of 0.92 mm, whereas the dry PEGel-2 beads have an average weight of 0.017 g and an average diameter of 1.40 mm.

The dry PEGel-1 and PEGel-2 beads were immersed in NaCl solutions with various salt concentrations. After fully swelling in the solutions at room temperature (27 °C) for 7 h, the PE gels reach the equilibrium volume. Then the images indicating the changes in size of the samples were recorded, as shown in Fig. 2. The Image Processing and Computer Vision Toolbox of Matlab (MathWorks Inc., MA)[27] was employed to trace the boundaries of the PE gels in the images for characterizations of the size. All the PE gels were considered as spheres, where the radius is r and the volume is $V = 4\pi r^3/3$.

RESULTS AND DISCUSSION

Scaling Laws for the Swelling Behavior

Analytical approximations

Considering that the salt ions are monovalent, we substitute $n_{\pm,\infty} = n_s$ into Eq. (3). Minimizing F_{elec} with respect to ψ and $n_\pm$, respectively, leads to the Poisson equation and Boltzmann distribution,

$$\frac{\delta F_{elec}}{\delta\psi} = 0 \Rightarrow \frac{d^2\psi}{dx^2} = \frac{e(-n_+ + n_-)}{\varepsilon_0\varepsilon_r} \tag{4a}$$

$$\frac{\delta F_{elec}}{\delta n_\pm} = 0 \Rightarrow \quad n_\pm = n_s \exp\left(\mp\frac{e\psi}{k_B T}\right) \tag{4b}$$

Minimizing F_{elec} with respect to ψ_s leads to the boundary condition at the charged surface,

$$\frac{\delta F_{elec}}{\delta\psi_s} = 0 \Rightarrow \left.\frac{d\psi}{dx}\right|_{x=\pm\ell} = \pm\frac{\sigma}{\varepsilon_0\varepsilon_r} \tag{5}$$

Since we have confirmed that the distance between the monomers are always smaller than the Debye length in the experiments, we can obtain the analytical approximations for ψ and $n_\pm$ using Eqs. (4a)–(5) considering $\lambda \gg \ell$,

$$\frac{e\psi(x)}{k_B T} \approx -\sinh^{-1}\left(\frac{\varphi}{2}\frac{N_t}{Vn_s}\right) - \frac{1}{2}\frac{\varphi}{\varphi_c}\left(\frac{x^2}{\ell^2} - \frac{1}{3}\right) \tag{6a}$$

$$n_\pm \approx \sqrt{\left(\frac{\varphi}{2}\frac{N_t}{V}\right)^2 + n_s^2} \mp \frac{\varphi}{2}\frac{N_t}{V} \tag{6b}$$

where $\varphi_c = a/(\pi\ell_B)$ is the critical charge fraction and $\ell_B = e^2/(4\pi\varepsilon_0\varepsilon_r k_B T)$ is the Bjerrum length.[25,26] Since we consider the scenario of overlapping EDLs, Eqs. (6a) and (6b) are consistent with the main results of the Donnan equilibrium.[23] Substituting Eqs. (6a) and (6b) into Eq. (3), we obtain the electrostatic free energy for the PE gel,

$$\frac{F_{elec}}{k_B T} \approx N_t\varphi\sinh^{-1}\left(\frac{\varphi N_t}{2n_s V}\right) + 2n_s V\left[1 - \sqrt{\left(\frac{\varphi N_t}{2n_s V}\right)^2 + 1}\right] \tag{7}$$

Substituting Eqs. (2) and (7) into Eq. (1) and minimizing F with respect to V, we obtain the swelling ratio at equilibrium considering two asymptotic conditions,

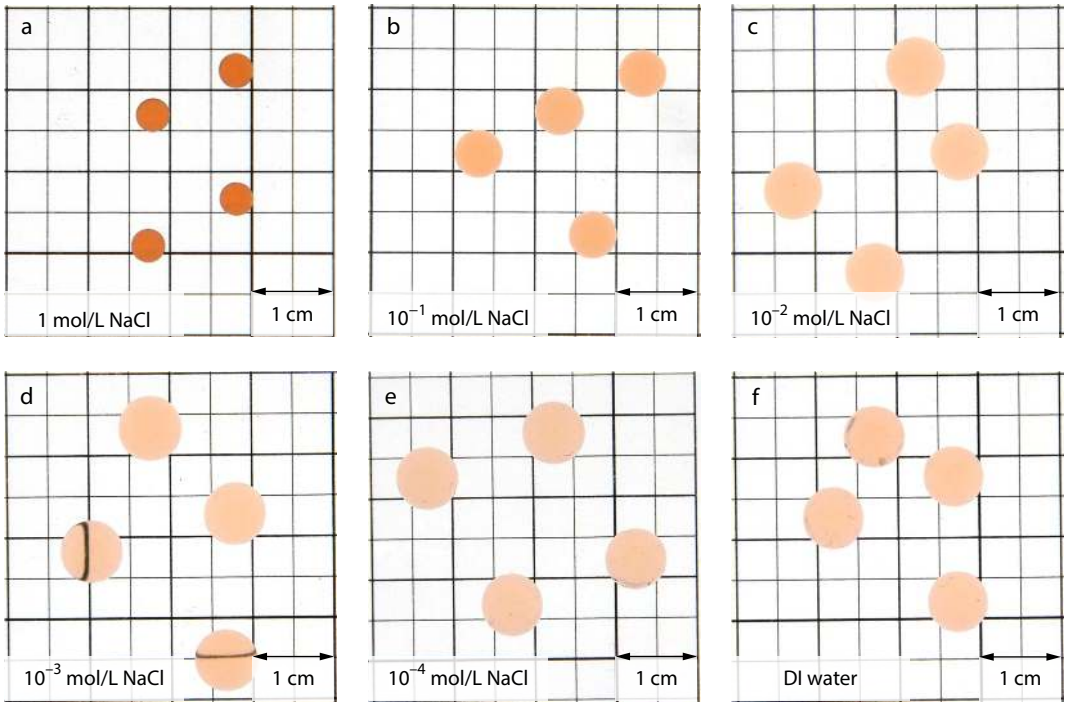

Fig. 2 Images of PEGel-1 after free swelling in (a–e) NaCl solutions of different concentrations and (f) DI water at room temperature (27 °C) for 7 h.

$$\frac{V}{V_0} \approx \left(\frac{k_B T n_{p,0}^2 \varphi^2}{4 G_0 n_s}\right)^{\frac{3}{5}}, \text{ for } \frac{n_{p,0}}{n_s} \ll 4\varphi^{\frac{1}{2}} \left(\frac{n_{p,0} k_B T}{G_0}\right)^{\frac{3}{2}} \quad (8a)$$

$$\frac{V}{V_0} \approx \left(\frac{k_B T n_{p,0} \varphi}{G_0}\right)^{\frac{3}{2}}, \text{ for } \frac{n_{p,0}}{n_s} \gg 4\varphi^{\frac{1}{2}} \left(\frac{n_{p,0} k_B T}{G_0}\right)^{\frac{3}{2}} \quad (8b)$$

where $n_p = N_t/V$ and $n_{p,0} = N_t/V_0$ are the monomer concentrations at equilibrium and at the reference state, respectively. We note that $V/V_0 \propto \varphi^{6/5} n_s^{-3/5}$ and $V/V_0 \propto \varphi^{3/2}$ predicted by Eqs. (8a) and (8b) are consistent with the power laws reported by Ref. [17,18]. However, our predictions are derived without *a priori* assumptions regarding the electroneutrality condition and salt ion components. As a result, our model can be directly employed to interpret the experimental data without the need for parameter fitting. Accordingly, the ratio between the the monomer concentrations at equilibrium n_p and at the reference state $n_{p,0}$ can be expressed as

$$\frac{n_p}{n_{p,0}} \approx \left(\frac{4 G_0 n_s}{k_B T n_{p,0}^2 \varphi^2}\right)^{\frac{3}{5}}, \text{ for } \frac{n_{p,0}}{n_s} \ll 4\varphi^{\frac{1}{2}} \left(\frac{n_{p,0} k_B T}{G_0}\right)^{\frac{3}{2}} \quad (9a)$$

$$\frac{n_p}{n_{p,0}} \approx \left(\frac{G_0}{k_B T n_{p,0} \varphi}\right)^{\frac{3}{2}}, \text{ for } \frac{n_{p,0}}{n_s} \gg 4\varphi^{\frac{1}{2}} \left(\frac{n_{p,0} k_B T}{G_0}\right)^{\frac{3}{2}} \quad (9b)$$

Comparisons and discussion

We compare the experimental measurements of the swelling ratio and monomer concentration with our numerical and analytical predictions.

The swelling ratios V/V_0 of PEGel-1 and PEGel-2 are plotted as a function of salt concentration n_s in Fig. 3(a). We define the reference state as the equilibrium state at n_s = 1 mol/L, where the swelling ratio is 1. The experimental data exhibit two distinct scaling behaviors with respect to n_s, which are well captured by our model using reasonable parameter values. Initially, the swelling ratio increases as n_s decreases, following the prediction $V/V_0 \propto n_s^{-3/5}$ by Eq. (8a). Subsequently, the swelling ratio reaches a plateau at low n_s, as predicted by Eq. (8b). PEGel-1 demonstrates a smaller swelling ratio compared to PEGel-2, particularly at low salt concentrations. It can be attributed to the fact that PEGel-1 has a relatively higher rigidity. The higher rigidity may be due to the larger number density of the cross-links within PEGel-1. Therefore, we anticipate that PEGel-1 has a larger shear modulus G_0 at the reference state, which in turn hinders the extent of swelling.

The data for PEGel-1 with higher rigidity exhibit a denser monomer distribution as compared to PEGel-2. The monomer concentrations n_p of PEGel-1 and PEGel-2 at equilibrium are plotted as a function of salt concentration n_s, as depicted in Fig. 3(b). The data points are obtained using the experimental observed volume V and the relationship $n_p = N_t/V$, which are well captured by our predictions. It is found that the monomer concentrations n_p of PEGel-1 are higher than those of PEGel-2 across all studied salt concentrations, especially at low salt concentrations. This observation further confirms our hypothesis that the higher rigidity of the PE gels lead to a denser monomer distribution as well as a smaller swelling ratio.

The dimensionless elastic free energy per monomer $F_{els}/(N_t k_B T)$ and dimensionless electrostatic free energy per monomer $F_{elec}/(N_t k_B T)$ at equilibrium for various salt concentration n_s are shown in Fig. 4. Apparently, $F_{els}/(N_t k_B T)$ and $F_{elec}/(N_t k_B T)$ increase simultaneously with decreasing n_s at high salt concentrations. When the swelling ratio approaches the maximum value at low n_s, the corresponding $F_{els}/(N_t k_B T)$ also tends to a maximum plateau. In contrast, $F_{elec}/(N_t k_B T)$

https://doi.org/10.1007/s10118-024-3152-2

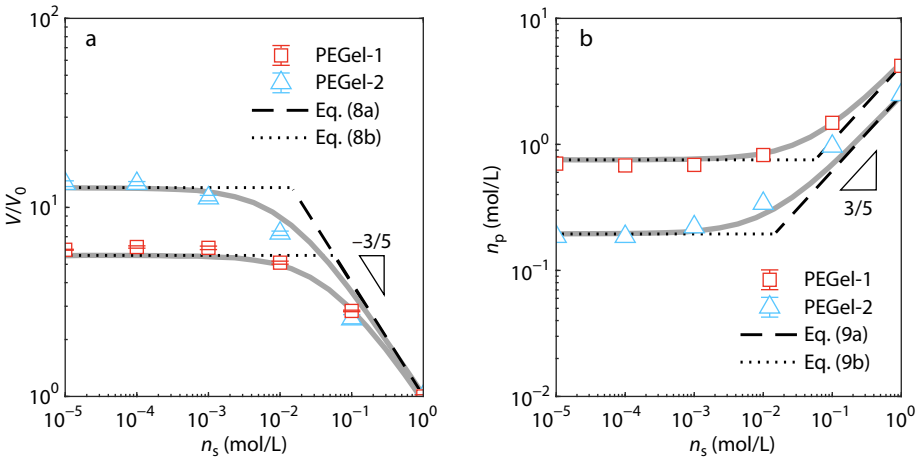

Fig. 3 (a) Swelling ratio V/V_0 and (b) monomer concentration n_p at equilibrium as functions of salt concentration n_s with the reference state defined as n_s = 1 M. The markers depict the experimental data. For the sake of representation, the experimental data corresponding to the DI water are shown at $n_s = 10^{-5}$ mol/L. The solid lines represent the numerical predictions considering $\varphi_c = 0.45$. The parameters for the PE gels are $N_t = 10^{20}$, $G_0 = 1$ MPa, $V_0 = 40$ mm^3, $\varphi = 0.3$ for PEGel-1, and $N_t = 3 \times 10^{20}$, $G_0 = 0.34$ MPa, $V_0 = 201$ mm^3, $\varphi = 0.3$ for PEGel-2. Other parameters for the solutions are $\varepsilon_0 = 8.8 \times 10^{-12}$ F/m, $\varepsilon_r = 80$, $k_B = 1.3804 \times 10^{-23}$ J/K and $T = 300$ K.

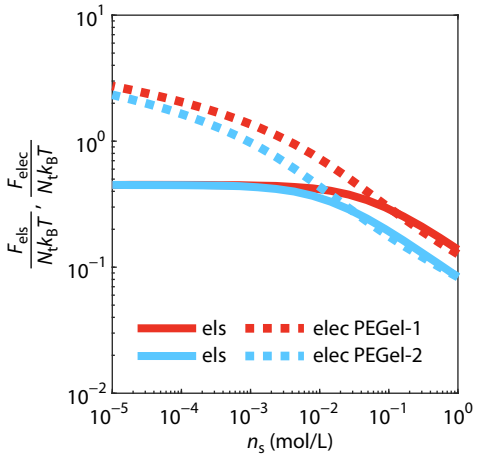

Fig. 4 Dimensionless elastic free energy per monomer $F_{els}/(N_t k_B T)$ and dimensionless electrostatic free energy per monomer $F_{elec}/(N_t k_B T)$ at equilibrium as functions of salt concentration n_s with the reference state defined as n_s = 1 M. The solid lines and dotted lines are the numerical predictions of $F_{els}/(N_t k_B T)$ and $F_{elec}/(N_t k_B T)$, respectively. The parameters are the same as those in Fig. 3.

continues to increase as n_s decreases, since the salt screening effect on the charged monomers is weakened at low salt concentrations. Therefore, we anticipate that, with the decrease of salt concentration, the mechanical properties of the PE gel are changing while the volume maintains constant.

Validity Verification of the Homogeneous Gel Assumption

Finite element model set up

The cell model, which is used to quantify the electrostatic energy of the PE gel, assumes a homogeneous distribution of monomers within the PE gel. Our recent work demonstrates that, as long as the size of the PE layer is much larger than the EDL thickness, the monomer distribution can be considered homogeneous.[28] This finding suggests that the homogeneous gel assumption is valid in this study, since the gel diameter (4−17 mm) is much larger than the Debye length (0.1−100 nm). To further demonstrate the validity of the cell model used in this study, we adopt a finite element (FE) model to simulate the electrostatic potential distribution, and thus to shed light on the monomer distribution within the PE gel.

In contrast to the cell model, which focuses on describing the electrostatic interactions between monomers, the FE model simulates the electrostatic interactions between the PE gel (orange part) and the external solution (blue part) on a macroscopic scale. The simulations are based on the mathematics branch of the COMSOL Multiphysics software (COMSOL AB).[29] The external NaCl solution is modelled as a cylindrical domain with a diameter of 20 cm and a height of 20 cm, as shown in Fig. 5. Since the size of the simulation box (*ca.* 20 cm) is sufficiently large compared to the Debye length (0.1−100 nm), the simulation results are not affected by the geometry of the simulation box. To facilitate visualization,

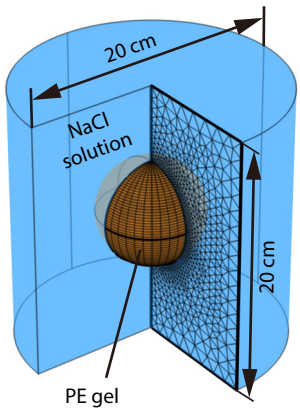

Fig. 5 Finite element model of a spherical PE gel immersed in a NaCl solution.

https://doi.org/10.1007/s10118-024-3152-2

1/4 of the solution domain is cut off to display the mesh. We probe the electrostatic potential ψ and local ion concentrations $n_{\pm}$ in the PE gel and external solution using the Poisson equation

$$\nabla^2\psi = \frac{e(n_- - n_+)}{\varepsilon_0\varepsilon_r}, \quad \text{for solution,} \tag{10a}$$

$$\nabla^2\psi = \frac{e(n_- - n_+)}{\varepsilon_0\varepsilon_r} + \frac{e\varphi n_p}{\varepsilon_0\varepsilon_r}, \quad \text{for gel,} \tag{10b}$$

and the Boltzmann distribution

$$n_{\pm} = n_s \exp\left(\mp\frac{e\psi}{k_B T}\right) \tag{11}$$

where the second term on the right-hand side of Eq. (10b) accounts for the contribution from the charged monomers. The boundaries (B) of the solution domain satisfy

$$(\boldsymbol{n}\cdot\nabla\psi)_B = 0 \tag{12}$$

The computations are carried out through the stationary solver.

Then, the electrostatic free energy F_{elec} of the PE gel is

$$\frac{F_{elec}}{k_B T} = \int_V -n_p\varphi\frac{e\psi}{k_B T}dV + \int_V -\frac{\varepsilon_0\varepsilon_r}{2k_B T}|\nabla\psi|^2 dV + \int_V\sum_i\left\{\frac{e\psi}{k_B T}z_i n_i + n_{i,\infty} + n_i\left[\ln\left(\frac{n_i}{n_{i,\infty}}\right) - 1\right]\right\}dV \tag{13}$$

The total free energy F of the PE gel is obtained by combining Eqs. (2) and (13). Subsequently, we employ the optimization solver to minimize the total free energy F with respect to the PE gel volume V, thereby determining V at equilibrium.

Comparisons and discussion

We generate the spatial distributions of the dimensionless electrostatic potential $e|\psi|/(k_B T)$ in the cross-sectional plane of both the PE gels and external solutions at equilibrium, considering different salt concentrations n_s. These results are depicted in the colormaps shown in Fig. 6 on the right panel, where the parameters used are consistent with Fig. 3. It is shown that the equilibrium sizes obtained by the simulations show perfect agreement with the experimental images on the left panel. The colorbar for $e|\psi|/(k_B T)$ with a maximum value of 8.67 is kept consistent across all the simulation results displayed in Fig. 6. The simulation results demonstrate that electrostatic potential $e|\psi|/(k_B T)$ within the gel increases as the salt concentration decreases, aligning with the observed increase in the electrostatic free energy with decreasing salt concentration shown in Fig. 4.

It is expected that the electrostatic potential ψ should be homogeneously distributed within the PE gel to ensure there is no internal electric field. It is shown in Fig. 6 that the value for the electrostatic potential is almost homogeneous inside the PE gel. The only spatial variation of ψ is observed near the interface between the PE gel and the external solution. The zoom-in illustration of the simulation result considering $n_s = 10^{-5}$ mol/L is shown in Fig. 7. We observe that the dimensionless electrostatic potential smoothly decreases from the maximum value (8.67) to the bulk value (0) across the gel-

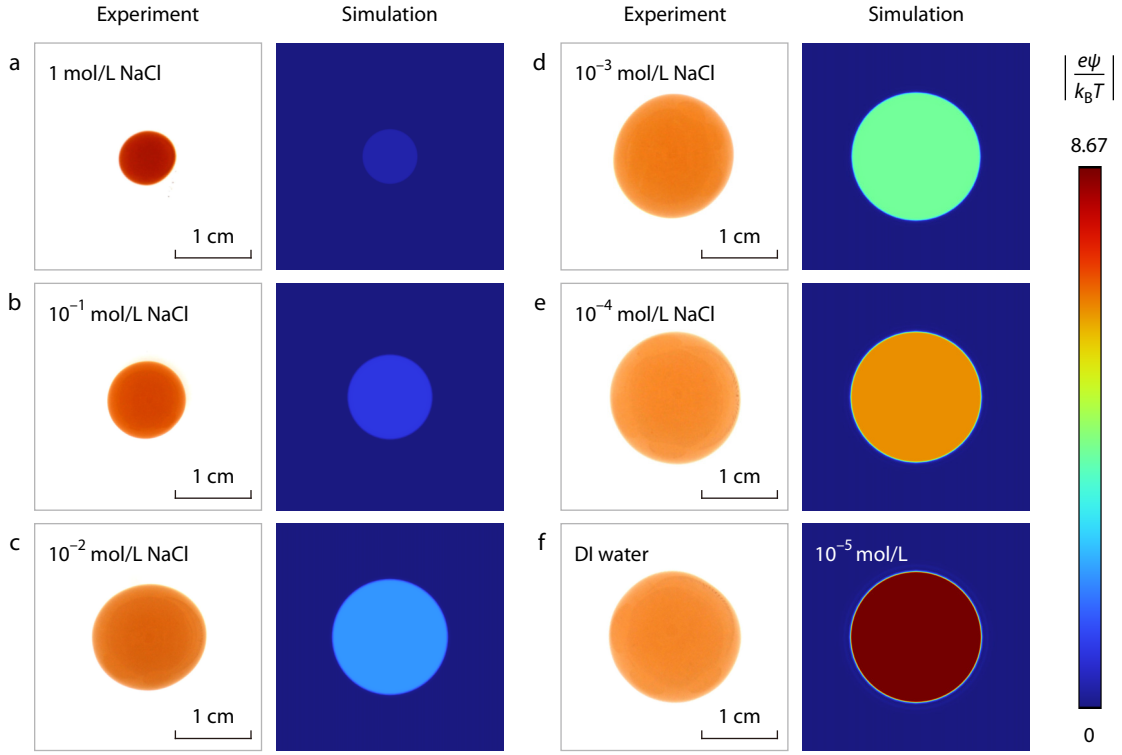

Fig. 6 Comparisons between experiments and FE simulations of the free swelling of PEGel-2 in (a–e) NaCl solutions of different concentrations and (f) DI water with the reference state defined as $n_s = 1$ mol/L. The simulation results present the spatial distributions of the dimensionless electrostatic potential $e|\psi|/(k_B T)$ in the PE gels and external solutions at equilibrium. A finite salt concentration $n_s = 10^{-5}$ mol/L is used in the simulation to compare with the experiment corresponding to the DI water. The parameters used are the same as those in Fig. 3.

https://doi.org/10.1007/s10118-024-3152-2

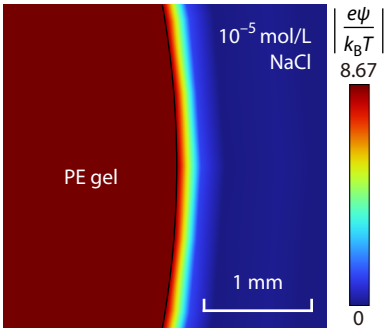

Fig. 7 Zoom-in illustration of the simulation result in Fig. 6(f) to depict the variation of the dimensionless electrostatic potential $e|\psi|/(k_BT)$ near the interface between the PE gel and the external solution.

solution interface. This variation only appears at a scale of 0.2 mm, whereas the corresponding PE gel diameter is 17 mm. It is confirmed that the size of the simulation box (*ca.* 20 cm) is sufficiently large in comparison with the scale of the potential variation (*ca.* 0.2 mm), ensuring the reliability of the simulation results. It is worth highlighting that the scale of the electrostatic potential variation for $n_s = 10^{-5}$ mol/L is the most pronounced among all the salt concentrations considered. Therefore, we confirm that the monomer distribution within the PE gel is hardly influenced by the small-scale variation of the electrostatic potential. However, we anticipate that the homogeneous gel assumption will break down for nanogels where the EDL thickness becomes comparable to the gel size.[28]

CONCLUSIONS

In this work, we develop a new theoretical model to understand the swelling behavior of spherical polyelectrolyte gels with added salt, which shows excellent agreement with the experimental characterizations for samples with different rigidities. In addition, we examine our theoretical results and the validity of homogeneous gel assumption *via* finite element simulations. The proposed cell model is also applicable to other PE systems with added salt, including semidilute PE solutions and PE brushes. We anticipate that our model shed light on multiple applications in biomedicine and advanced manufacturing, such as drug adsorption and release, deformation of red blood cells, 4D printing and soft robotics, where the underlying mechanism of swelling remains enigmatic.

Conflict of Interests

The authors declare no interest conflict.

Data Availability Statement

The data that support the findings of this study are available from the corresponding author upon reasonable request.

ACKNOWLEDGMENTS

This work was financially supported by the National Natural Science Foundation of China (No. 12372259).

REFERENCES

1 Kwon, H. J.; Osada, Y.; Gong, J. P. Polyelectrolyte gels: fundamentals and applications. *Polym. J.* **2006**, *38*, 1211–1219.
2 Ahn, S. K.; Kasi, R. M.; Kim, S. C.; Sharma, N.; Zhou, Y. Stimuli-responsive polymer gels. *Soft Matter* **2008**, *4*, 1151–1157.
3 White, E. M.; Yatvin, J.; Grubbs, J. B.; Bilbrey, J. A.; Locklin, J. Advances in smart materials: Stimuli-responsive hydrogel thin films. *J. Polym. Sci., Part B: Polym. Phys.* **2013**, *51*, 1084–1099.
4 Mirvakili, S. M.; Hunter, I. W. Artificial muscles: mechanisms, applications, and challenges. *Adv. Mater.* **2018**, *30*, 1704407.
5 Park, N.; Kim, J. Hydrogel-based artificial muscles: overview and recent progress. *Adv. Intell. Syst.* **2020**, *2*, 1900135.
6 Lin, W. C.; Yu, D. G.; Yang, M. C. pH-sensitive polyelectrolyte complex gel microspheres composed of chitosan/sodium tripolyphosphate/dextran sulfate: swelling kinetics and drug delivery properties. *Colloids Surf. B* **2005**, *44*, 143–151.
7 Cazorla-Luna, R.; Martin-Illana, A.; Notario-Perez, F.; Ruiz-Caro, R.; Veiga, M. D. Naturally occurring polyelectrolytes and their use for the development of complex-based mucoadhesive drug delivery systems: An overview. *Polymers* **2021**, *13*, 2241.
8 Champeau, M.; Heinze, D. A.; Viana, T. N.; de Souza, E. R.; Chinellato, A. C.; Titotto, S. 4D printing of hydrogels: a review. *Adv. Funct. Mater.* **2020**, *30*, 1910606.
9 Zolfagharian, A.; Denk, M.; Bodaghi, M.; Kouzani, A. Z.; Kaynak, A. Topology-optimized 4D printing of a soft actuator. *Acta Mech. Solida Sin.* **2020**, *33*, 418–430.
10 Flory, P. J.; Rehner, J. Statistical mechanics of cross-linked polymer networks i. Rubberlike elasticity. *J. Chem. Phys.* **1943**, *11*, 512–520.
11 Flory, P. J.; Rehner, J. Statistical mechanics of cross-linked polymer networks ii. Swelling. *J. Chem. Phys.* **1943**, *11*, 521–526.
12 Tanaka, T. Collapse of gels and the critical endpoint. *Phys. Rev. Lett.* **1978**, *40*, 820–823.
13 Donnan, F. G. The theory of membrane equilibria. *Chem. Rev.* **1924**, *1*, 73–90.
14 Flory, P. J. *Principles of polymer chemistry*. Cornell university press: USA, **1953,** p. 584.
15 Ohmine, I.; Tanaka, T. Salt effects on the phase transition of ionic gels. *J. Chem. Phys.* **1982**, *77*, 5725–5729.
16 Ricka, J.; Tanaka, T. Swelling of ionic gels: quantitative performance of the donnan theory. *Macromolecules* **1984**, *17*, 2916–2921.
17 Skouri, R.; Schosseler, F.; Munch, J. P.; Candau, S. J. Swelling and elastic properties of polyelectrolyte gels. *Macromolecules* **1995**, *28*, 197–210.
18 Rubinstein, M.; Colby, R. H.; Dobrynin, A. V.; Joanny, J. F. Elastic modulus and equilibrium swelling of polyelectrolyte gels. *Macromolecules* **1996**, *29*, 398–406.
19 Hong, W.; Zhao, X.; Suo, Z. Large deformation and electrochemistry of polyelectrolyte gels. *J. Mech. Phys. Solids* **2010**, *58*, 558–577.
20 Hua, J.; Mitra, M. K.; Muthukumar, M. Theory of volume transition in polyelectrolyte gels with charge regularization. *J. Chem. Phys.* **2012**, *136*, 134901.
21 Jia, D.; Muthukumar, M. Interplay between microscopic and macroscopic properties of charged hydrogels. *Macromolecules* **2020**, *53*, 90–101.
22 Jia, D.; Muthukumar, M. Theory of charged gels: Swelling, elasticity, and dynamics. *Gels* **2021**, *7*, 49.

23 Doi, M. *Soft matter physics*. Oxford University Press: USA, **2013** p 38.
24 Tang, J.; Katashima, T.; Li, X.; Mitsukami, Y.; Yokoyama, Y.; Chung, U. I.; Shibayama, M.; Sakai, T. Effect of nonlinear elasticity on the swelling behaviors of highly swollen polyelectrolyte gels. *Gels* **2021**, *7*, 25.
25 Chen, G.; Perazzo, A.; Stone, H. A. Influence of salt on the viscosity of polyelectrolyte solutions. *Phys. Rev. Lett.* **2020**, *124*, 177801.
26 Chen, G.; Perazzo, A.; Stone, H. A. Electrostatics, conformation, and rheology of unentangled semidilute polyelectrolyte solutions. *J. Rheol.* **2021**, *65*, 507−526.
27 *MATLAB* version 9.13.0 (R2022b), The MathWorks Inc., Natick, Massachusetts, United States.
28 Duan, M.; Chen, G. Swelling and shrinking of two opposing polyelectrolyte brushes. *Phys. Rev. E* **2023**, *107*, 024502.
29 *COMSOL Multiphysics* version 6.1, COMSOL AB, Stockholm, Sweden.

https://doi.org/10.1007/s10118-024-3152-2